Arch. Metall. Mater. **71** (2026), 1, 17-24

DOI: https://doi.org/10.24425/amm.2026.157765

VENU GOPAL RAO SIRUVOLU[1*], AHMED ABDULLAH AAFAQ[2], NAGENDRA SINGH[3], PANKAJ KUMAR[4], AKSHAY GANPAT TAJANE[5], BEPORAM IFTEKHAR HUSSAIN[6]

EFFECT OF THERMAL CONDITIONS ON THE TRIBOLOGICAL CHARACTERISTICS OF HYPOEUTECTIC SPHEROIDAL AND COMPACTED GRAPHITE IRONS

This study examines the sliding wear behavior of hypoeutectic spheroidal graphite iron (SGI) and compacted graphite iron (CGI) under different thermal conditions, focusing on their potential for high-temperature tribological applications. Samples of SGI and CGI with varying magnesium content were synthesized and subjected to both rotary and linear reciprocating wear tests at temperatures ranging from room temperature to 500°C. The wear loss and frictional forces were analyzed in detail using scanning electron microscopy (SEM) and energy-dispersive X-ray spectroscopy (EDX). The results demonstrate distinct tribological responses between SGI and CGI, governed by graphite morphology and microstructural stability at elevated temperatures. CGI showed enhanced thermal stability and crack resistance due to its coral-like graphite structure, while SGI exhibited superior ductility and moderate wear resistance.

Keywords: Tribology; Cast Iron; Composites; Melting; Heat Treatment

1. Introduction

Cast iron continues to be one of the most important industrial materials worldwide, accounting for around 70% of all castings manufactured globally across its different types. [1]. This dominance is largely due to its excellent mechanical and thermal properties, combined with its low production cost. Cast iron is essentially an alloy of iron and carbon, typically containing 2-4 wt.% carbon (either as carbide or graphite), along with 1-3 wt.% silicon [2].

Among the different types, ductile iron – also known as spheroidal or nodular graphite iron – makes up about 20-30% of total cast iron production [3]. In this variety, graphite appears as small, spherical nodules dispersed throughout the metal matrix, resulting in better matrix continuity compared to grey or compacted graphite irons. This morphology significantly enhances mechanical properties, as the nodular graphite structure effectively arrests cracks, making ductile iron stronger than its flake or compacted graphite counterparts. The formation of these nodules is typically promoted by adding small amounts of spheroidizing elements such as magnesium (around 0.04-0.06%).

The key factors that influence the properties of cast iron include variations in its main constituents – carbon, silicon, and iron – along with casting technique, melting temperature, and any post-processing heat treatments. Another important variant, compacted graphite iron (CGI), exhibits unique mechanical and physical characteristics that lie between those of flake and nodular graphite irons. In CGI, the graphite forms short, stubby particles with rounded edges that cluster together, creating a "vermicular" or "compacted" structure. The term "compacted" is preferred as it better captures the three-dimensional nature of the graphite morphology.

Both spheroidal graphite cast iron and compacted graphite iron are considered part of the binary Fe-C system, typically containing over 2% carbon and 1-3% of elements such as manganese and silicon. Other elements like phosphorus and sulfur are usually present in smaller quantities [4]. To achieve specific physical, mechanical, or tribological characteristics, cast irons can be alloyed with elements such as manganese, nickel, and silicon [5,6]. These additions influence the size, shape, and distribution of graphite, as well as the type of metallic matrix [7-9].

[1] DEPARTMENT OF MECHANICAL ENGINEERING, DRK INSTITUTE OF SCIENCE AND TECHNOLOGY, INDIA
[2] DEPARTMENT OF MECHANICAL ENGINEERING, B.S. ABDUR RAHMAN CRESCENT INSTITUTE OF SCIENCE AND TECHNOLOGY, VANDALUR, CHENNAI, TAMIL NADU, INDIA
[3] DEPARTMENT OF MECHANICAL ENGINEERING, INSTITUTE OF ENGINEERING AND TECHNOLOGY, KHANDARI CAMPUS, AGRA, UP, INDIA
[4] DEPARTMENT OF MECHANICAL ENGINEERING, CHANDIGARH UNIVERSITY, PUNJAB, INDIA
[5] DEPARTMENT OF MECHANICAL ENGINEERING, SANDIP UNIVERSITY, NASHIK, MAHARASHTRA, INDIA
[6] DEPARTMENT MECHANICAL ENGINEERING, BAPATLA ENGINEERING COLLEGE, BAPATLA, ANDHRA PRADESH, INDIA

* Corresponding author: svgrao1@gmail.com

In some cases, heat treatments like austempering [10,11] are used to tailor the microstructure for specific applications. For instance, during eutectoid transformation, pearlite forms – consisting of alternating layers of ferrite and cementite. Pearlite is stronger than ferrite due to this lamellar arrangement. At 727°C, the maximum carbon solubility in ferrite is about 0.02%, and this decreases sharply at lower temperatures [8].

Alloying elements are broadly classified based on whether they stabilize ferrite or pearlite. Elements like Mn, Cu, Ni, and N favor pearlite formation, while Cr, Nb, Mo, Ti, and Si tend to stabilize ferrite [7,8]. Cooling rate also significantly affects the microstructure: faster cooling results in finer pearlite, which enhances strength by reducing interlamellar spacing [12]. Pearlitic cast irons are often used in applications that demand high stiffness, excellent damping, and a good surface finish. In contrast, pure ferritic irons have limited use due to their lower strength. As the proportion of ferrite increases relative to pearlite, both strength and hardness typically decline [8-13]. However, pearlitic cast irons, while stronger, are more difficult to machine due to their heterogeneous hardness, making ferritic cast irons more suitable for applications where machinability is critical.

Tribology – the study of friction, wear, and lubrication – is central to understanding the performance and durability of cast iron components, particularly in automotive and industrial contexts. SGI and CGI are especially valued for their mechanical strength, cost-effectiveness, and customizable tribological properties. The wear behavior of cast iron is closely tied to its matrix structure and the morphology of the graphite. The graphite acts as a solid lubricant, forming a protective layer that lowers friction and wear during sliding contact. This self-lubricating behavior helps maintain a steady graphite presence on the contact surface, reducing direct metal-to-metal contact and resulting in lower wear rates [14].

In a detailed study, Riahi et al. [15] examined the wear performance of lamellar cast iron under dry sliding conditions, simulating poor lubrication scenarios with varying loads and speeds. They found that graphite disperses onto the sliding surface, forming a thin lubricating film that helps reduce wear [16,17]. Sugishita et al. [14,18] also highlighted the tribological advantages of exposed graphite on sliding surfaces. Despite numerous studies, there is limited comparative research focused on simultaneously optimizing wear loss and frictional forces for both SGI and CGI.

Therefore, the present study aims to fill this gap by evaluating the comparative wear and friction behavior of SGI and CGI under rotary as well as linear wear conditions, at ambient as well as elevated temperatures. Special emphasis is placed on the influence of microstructure and graphite morphology on their tribological performance.

2. Materials and methodology

2.1. Fabrication of SG and CG Iron

Steel scrap and pig iron serve as the primary raw materials for the production of both spheroidal graphite (SG) iron and compacted graphite (CG) iron. The melting process is carried out using an induction furnace with a 1-ton capacity and a maximum attainable temperature of 3027°C. The scrap iron is melted to a liquid state at around 1538°C. During melting, alloying elements such as silicon and manganese are introduced in the form of ferroalloys to achieve the desired chemical composition (Fig. 1).

Fig. 1. Iron melting induction furnace Stir Casting of Nanocomposites

Magnesium treatment is a critical step in controlling the morphology of graphite. Magnesium is added to the molten metal in the form of a Fe-Si-Mg master alloy. The amount of magnesium added determines whether SG or CG iron is produced. For SG iron, a higher magnesium content (approximately 0.05%) promotes the formation of spherical graphite nodules. In contrast, a lower magnesium content (around 0.02%) reduces the degree of nodularity, resulting in the formation of vermicular or compacted graphite, characteristic of CG iron. The optimal temperature range for magnesium treatment lies between 1526°C and 1626°C.

A mold cavity is formed using a two-part pattern measuring $305 \times 205 \times 45$ mm^3. Green sand serves as the molding material, and carbon dioxide gas is applied to harden the mold. The green sand mold is maintained at an approximate strength of 80 kN/m^2.To enhance the cohesion strength of the mold, fine sand is mixed with special binders, clay, and water.

After melting, the treated molten metal is poured into the prepared mold cavity. The timing and control of magnesium treatment are critical – especially since final Mg additions can be made just before or during pouring to achieve the required graphite structure. The resulting microstructure can be further modified through appropriate heat treatment, enabling control over the matrix structure for targeted mechanical properties. SG iron contains nodular graphite, while CG iron exhibits graphite in a vermicular or compacted form due to the lower Mg content and controlled solidification. The fabricated samples were analyzed for their chemical composition as mentioned in TABLES 1 and 2.

The Microstructural examination of both the SG and CG Iron was carried out as represented in Fig. 2. The samples of SG iron and CG iron were polished and the microstructures are studied after proper etching.SG Iron microstructure consists

TABLE 1

Chemical composition of SG Iron

Fe	C	Si	Mn	P	S	Mg	Mo
93.75	3.61	2.21	0.33	0.041	0.0021	0.05	0.001

TABLE 2

Chemical composition of CG Iron

Fe	C	Si	Mn	P	S	Mg	Mo
93.78	3.61	2.21	0.33	0.041	0.0021	0.02	0.001

of spherical graphite with ferrite and pearlite matrix. Pearlite is two phased, layered structure with alternating layers of ferrite and cementite. Microstructure of CG iron consists of vermicular graphite in the matrix of ferrite and pearlite.

2.2. Heat Treatment

The microstructure of SG iron and CG iron can be altered through heat treatment. In this study, both materials undergo an austempering process. Cylindrical specimens with a diameter of 10 mm and a length of 15 mm are extracted from castings using Electrical Discharge Machining (EDM). These specimens are heated to 860°C, held at that temperature for one hour, and then quenched in a salt bath maintained at 250°C for 60 minutes, followed by air cooling to ambient temperature. The complete heat treatment process is illustrated in Fig. 3.

2.3. Wear analysis

Wear behavior of SG iron and CG iron is evaluated using two different tribological test methods: a Pin-on-Disc tribometer for assessing rotary wear and a linear reciprocating tribometer for analyzing sliding wear. Cylindrical test specimens, each measuring 10 mm in diameter and 15 mm in height, are extracted from the SG and CG iron castings and used as pin materials. The disc counterpart is made of High Carbon-High Chromium steel. Rotary wear tests are performed using the Pin-on-Disc tribometer under both ambient and elevated temperature conditions (100°C, 200°C, 300°C, and 500°C), following **ASTM G99** testing standards. Similarly, the linear wear performance is assessed using a reciprocating tribometer under the same temperature conditions, with the same specimen dimensions and disc material.

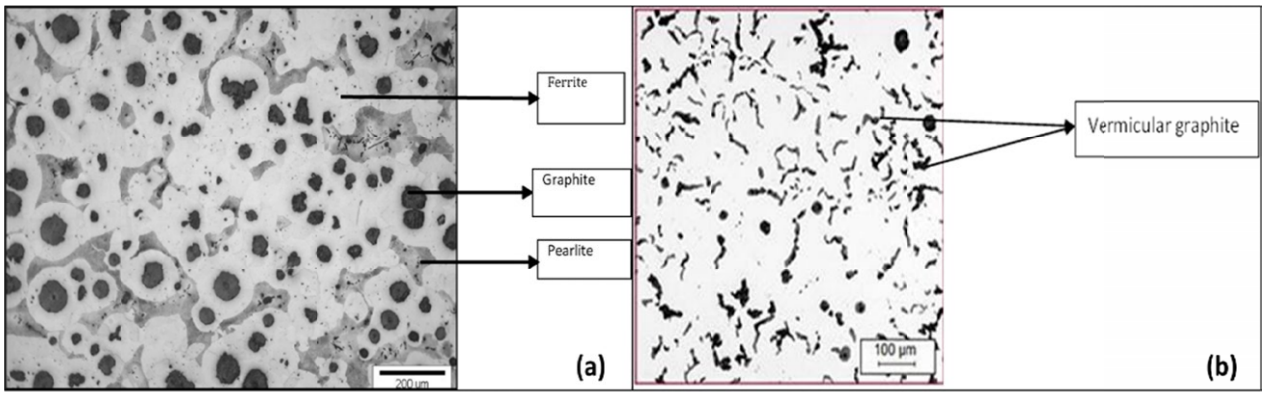

Fig. 2. a) SG Iron microstructure b) CG Iron microstructure with vermicular graphite

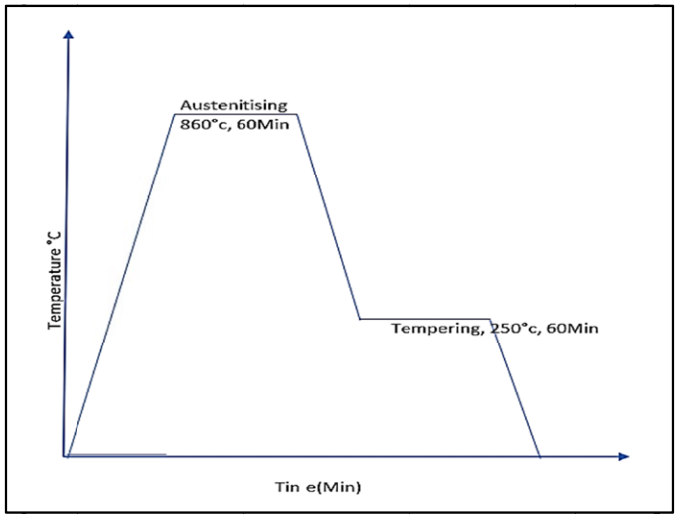

Fig. 3. Austempering heat treatment cycle

3. Results and discussions

3.1. Microstructural Analysis

When observed under an optical microscope, spheroidal graphite (SG) iron displays a clean and uniform microstructure, where the graphite appears as small, rounded black nodules evenly distributed throughout the metallic matrix, Fig. 4a). These nodules are formed by the addition of magnesium during the melting process, which promotes the spherical shape of graphite [19,20]. This nodular form is highly beneficial, as it minimizes stress concentration and helps prevent crack propagation, contributing to the superior strength and toughness of SG iron [21]. The surrounding matrix typically consists of a combination of ferrite and pearlite – ferrite providing ductility and pearlite offering strength – resulting in a balanced mechanical performance [22].

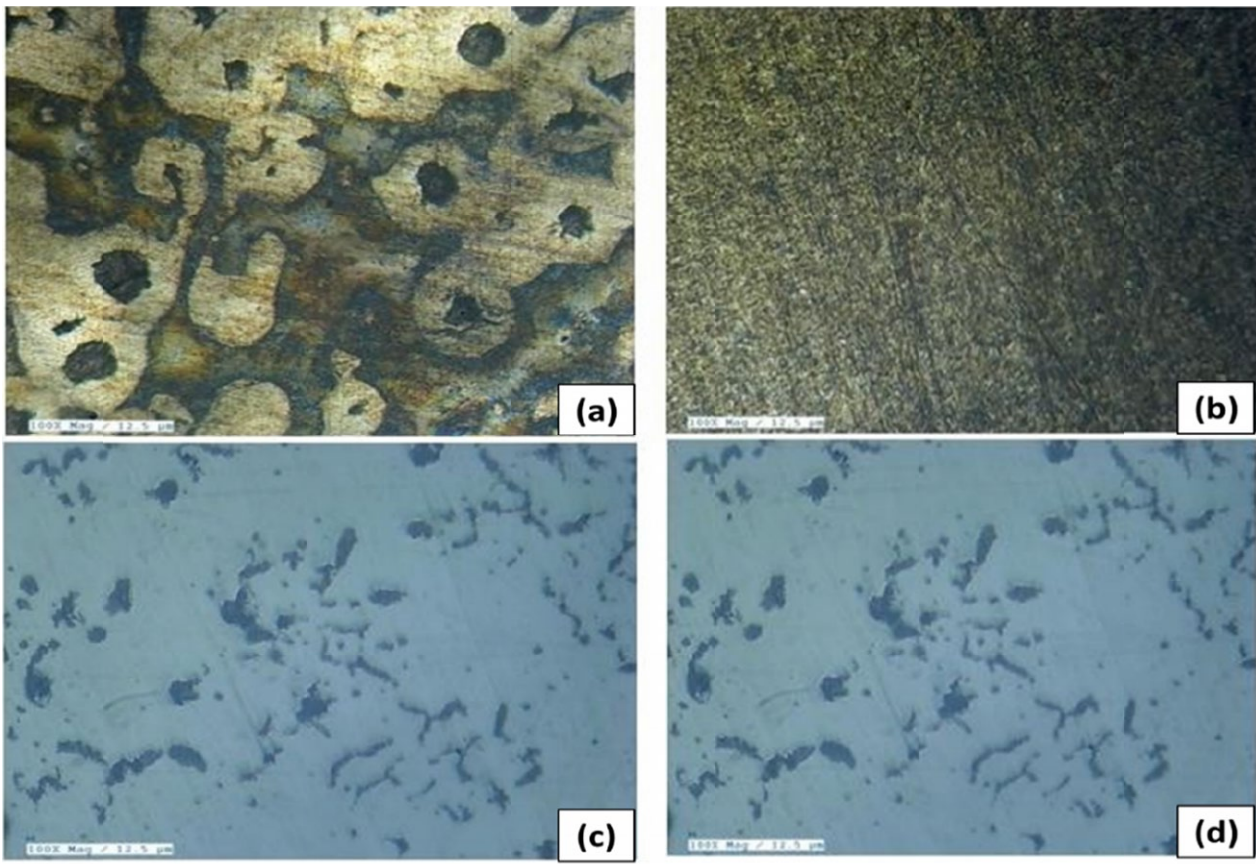

Fig. 4. a) Microstructure of as cast SG iron casting with 0.05% Mg, b) Microstructure of austempered SG Iron with 0.05% Mg, c) Microstructure of as cast CG iron with 0.02% Mg, d) Microstructure of austempered CG Iron with 0.02% Mg

In contrast, compacted graphite (CG) iron exhibits a markedly different graphite structure, Fig. 4b). Instead of round nodules, the graphite takes on a short, thick, curved, worm-like form known as vermicular graphite [23]. This structure is achieved by carefully controlling the magnesium content to a lower level than in SG iron [24]. Under the microscope, CG iron's graphite appears partially interconnected, and the matrix generally comprises ferrite and pearlite as well [25]. While it lacks the ductility of SG iron, CG iron offers a favorable combination of strength, thermal conductivity, and damping capacity, making it ideal for applications where both mechanical and thermal performance are important [26]. The most prominent visual difference between SG and CG iron under optical microscopy lies in the graphite morphology: spherical in SG iron and vermicular in CG iron.

Austempering has a notable impact on modifying the matrix structure of both spheroidal graphite iron and compacted graphite iron.While the graphite morphology – spheroidal in SG iron and vermicular in CG iron – remains unchanged during the heat treatment, the surrounding matrix undergoes a notable transformation. Austempering replaces the conventional ferrite-pearlite matrix with a bainitic structure, commonly referred to as an ausferritic matrix, which consists of a mix of acicular ferrite and high-carbon stabilized austenite [27,28], shown in Figs. 4c) and 4d). Under an optical microscope, this transformed matrix appears darker and more refined compared to untreated structures, giving the material enhanced strength, toughness, and wear resistance [29]. This binate (dual-phase) microstructure – formed through controlled heat treatment and isothermal holding – greatly improves the mechanical performance of both materials, making austempered spheroidal graphite iron (ADI) and austempered compacted graphite iron (ACGI) suitable for demanding applications where conventional cast irons may not perform as effectively [30,31].

3.2. Wear analysis of SG iron

Two types of wear analyses were conducted, one is the rotary sliding wear analysis and the other is the linear sliding wear analysis for both SG and CG iron specimens under various temperatures such as room temperature and at elevated temperatures i.e. 100°C, 200°C, 300°C and 500°C.Pin on disc tribometer is used in investigations for rotary wear. In the case of rotary wear, it is observed that the wear loss of SG iron consistently increases with time at all temperatures, Fig. 5. Initially, the wear rate is relatively low, but it begins to rise sharply after about 5 minutes of operation. This trend is mirrored in the behavior of frictional forces, which also increase over time. At elevated temperatures – particularly at 500°C(2.8×10^{-4} $mm^3/N \cdot m$), – the rate of increase in both wear and friction is more pronounced. This can be attributed to the formation of oxide layers on the surface, which influence the wear mechanism. SEM images

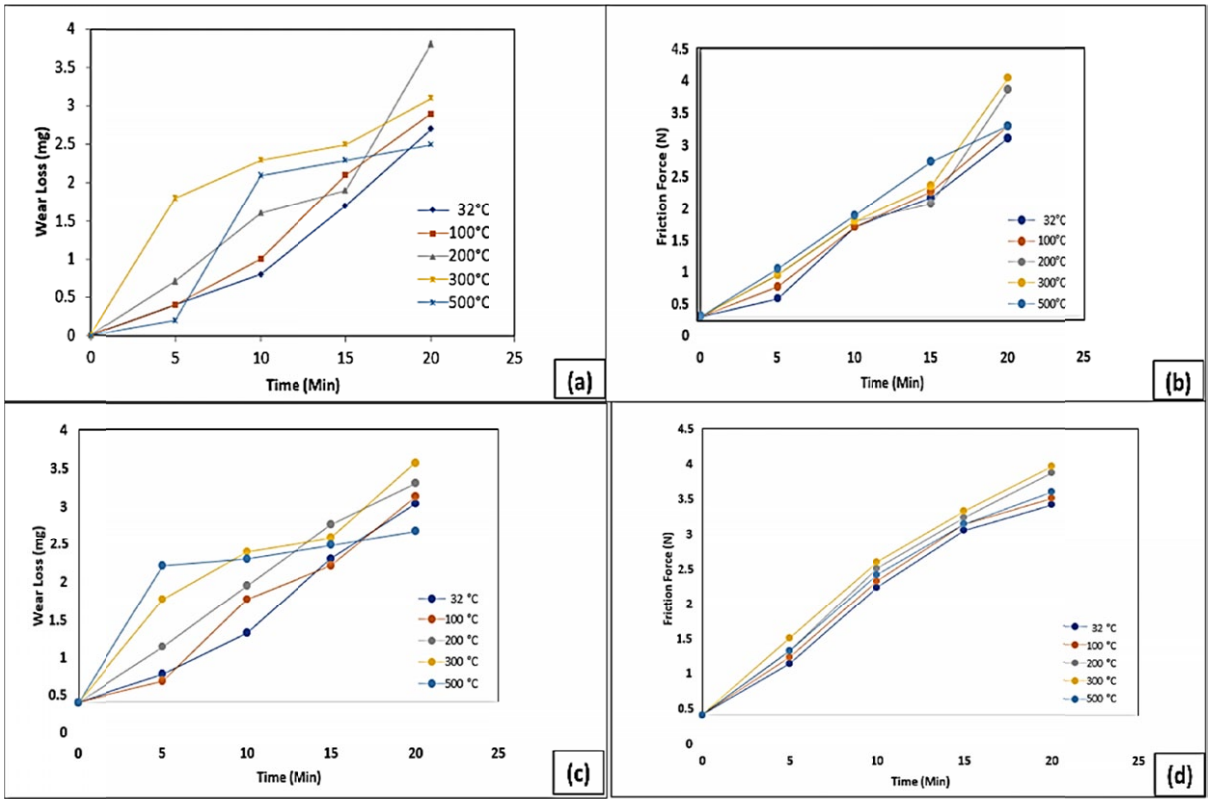

Fig. 5. a) SG Iron rotary wear loss (mg) with 0.05% Mg at various temperatures, b) SG Iron Rotary Frictional Forces (N) with 0.05% Mg at various temperatures, c) Linear wear loss (in mg) of SG Iron containing 0.05% Mg measured at different temperatures, d) Linear Frictional Forces (N) of SG Iron with 0.05% Magnesium at Different Temperatures

support this observation, showing that wear scars are less severe at room temperature in SG iron containing 0.05 wt.% magnesium. The figures (Figs. 5a, 5b) clearly indicate that wear loss continues to rise with time and becomes more significant as the temperature increases. However, beyond 15 minutes, although wear continues to increase, the rate at which it does so begins to taper off, especially at 500°C. This may be due to thermal softening of the material, which could lead to localized adhesion of pin material to disc surface, thereby reducing the incremental wear rate. Meanwhile, frictional forces continue to grow steadily, and their rate of increase becomes even more noticeable beyond 15 minutes at high temperatures like 500°C, further highlighting the complex interaction between temperature, surface oxidation, and material behavior during prolonged wear.

As given in Figs. 5c, 5d, under linear wear conditions, wear loss increases steadily with time for all levels of magnesium content. However, it is consistently observed that the wear loss under linear motion is greater than that under rotary conditions. A sharp increase in wear occurs particularly after the first 5 minutes. This initial phase likely involves the removal of surface microirregularities, which leads to more intimate contact between the pin and disc surfaces. As the wear depth increases over time, the actual contact area may begin to reduce slightly, resulting in a slower rate of wear beyond the 15-minute mark. A similar trend is observed in frictional forces, which also rise with time (Fig. 5d). At higher temperatures, especially around 500°C, the increase in friction becomes more pronounced, largely due to the formation of surface oxide layers [32,33]. At moderate temperatures between 100°C and 300°C, the frictional force curves are relatively flatter, indicating a more gradual increase. Overall, wear loss continues to rise at all temperatures as a function of time, with the highest rate of wear occurring in the initial 5 minutes, particularly at elevated temperatures. Beyond this point, the wear rate begins to level off. At 500°C, the wear-time curve becomes nearly flat, likely due to softening of the pin material, which may lead to localized sticking to the disc surface and a subsequent stabilization of wear. Frictional forces follow a similar pattern – increasing with temperature and showing a higher rate of increase after 15 minutes, especially at 500°C, where oxide layer formation contributes to the elevated friction.

3.3. Wear analysis of CG iron

The wear behavior of compacted graphite (CG) iron was analyzed at both room temperature and elevated temperatures, using experimental measurements of wear loss and frictional force. Tests were conducted separately under rotary and linear sliding conditions for CG iron castings containing 0.02 wt.% magnesium. The results show that, under rotary wear, wear loss steadily increases with time at all temperatures. However, unlike SG iron, CG iron exhibits a relatively higher wear rate during the initial stages, especially within the first 5 minutes. After

this period, the rate of wear tends to slow down, and beyond 15 minutes, the trend becomes similar to that observed in SG iron. As expected, wear loss increases with temperature, with a noticeable rise up to 300°C. At 500°C, the wear-time curve begins to flatten, indicating a stabilization in wear rate. This behavior may be attributed to thermal softening and the formation of oxide layers on the surface.

Frictional forces follow a similar time-dependent pattern. They increase steadily at all temperatures, but the rate of increase varies. At 500°C, the frictional force curve becomes significantly steeper compared to other temperatures, likely due to the formation of oxide layers that increase surface interaction. This trend is consistent across different levels of magnesium content. While the wear rate generally decreases beyond the initial 5 minutes, friction continues to build, particularly at higher temperatures. The findings of this study align well with the observations reported by Shaha et al. [34], and the role of oxide formation in influencing friction at elevated temperatures, especially around 500°C, is also supported by prior literature [35].

Under linear sliding wear conditions, compacted graphite (CG) iron shows greater wear loss compared to rotary wear. Across all tested temperatures, CG iron containing 0.02% magnesium records the highest levels of wear.Notably, CG iron with a lower magnesium content of 0.008% shows a more rapid increase in wear rate, particularly after the first 5 minutes of testing. During this initial phase, surface micro-irregularities on both the pin and disc are worn away, resulting in better contact between the mating surfaces. As wear progresses and deeper scars develop, the actual contact area may decrease slightly, leading to a reduced rate of wear beyond the 15-minute mark.

Frictional forces display a similar trend over time, with a slight variation observed at the elevated temperature of 500°C. At room temperature, both wear loss and the severity of wear scars are relatively low when compared to results at 200°C and 500°C. Ingeneral, wear loss increases with time at all temperatures, but the rate of increase varies. As the temperature rises, wear loss increases up to about 300°C. Beyond this point, however, wear loss tends to decrease, possibly due to changes in material behavior or oxide layer formation. After the first 5 minutes, the rate of wear slows down across all temperatures, with the wear-time curve appearing nearly flat at 300°C. Oxidative wear at 300°C, transitioning to oxidative-abrasive wear at 400°C and severe delamination and oxide spallation at 500°C. EDX spectra confirming oxide layer composition (Fe_2O_3, Fe_3O_4).

These findings are consistent with those reported by Shaha et al. [34], confirming the observed wear patterns. Frictional forces also increase with time, though the rate of increase differs across temperatures. At 500°C, the frictional force curves become significantly steeper, indicating a sharp rise in friction. This can be attributed to the formation of oxide layers at higher temperatures [35], which may contribute to increased resistance at the contact interface.

Compacted graphite (CG) iron demonstrates greater wear loss and higher frictional forces than spheroidal graphite (SG) iron under both rotary and linear wear conditions, consistent with the results reported by Hirasata et al. [36]. Furthermore, for both

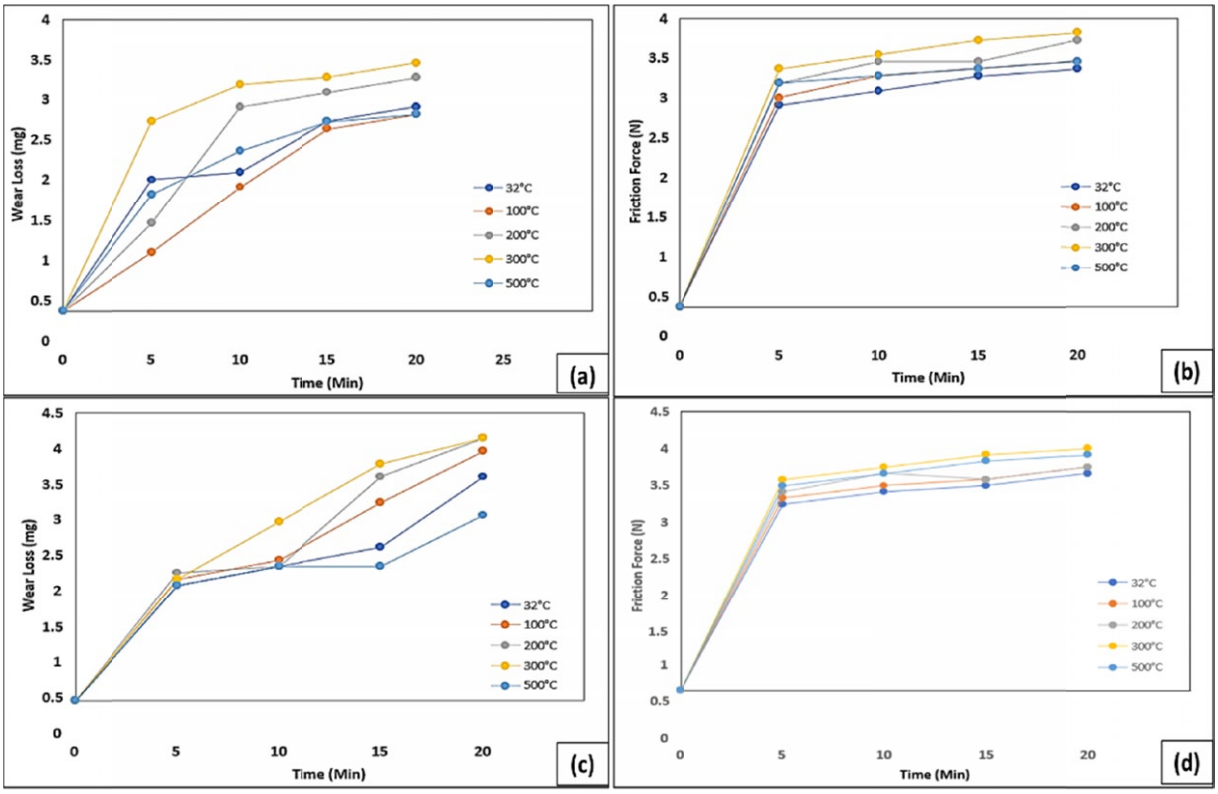

Fig. 6. a) Rotary Wear Loss (mg) of CG Iron Containing 0.02% Magnesium at Various Temperatures, b) Rotary Frictional Forces (N) of CG Iron with 0.02% Magnesium at Different Temperatures, c) Linear Wear Loss (mg) of CG Iron with 0.02% Magnesium at Various Temperatures, d) Linear Frictional Forces (N) of CG Iron with 0.02% Magnesium at Various Temperatures

CG and SG iron, wear loss is consistently higher during linear sliding wear than during rotary wear. The increase in wear rate is also more pronounced in linear wear compared to rotary conditions. A similar pattern is noted for frictional forces, which tend to rise more sharply under linear conditions, indicating a stronger interaction at the contact surfaces during reciprocating motion, it is also observed that at 400°C, SGI exhibited approximately 28% lower wear loss compared to CGI, while at 500°C the difference increased to 36%.

5. Conclusions

This study focuses on the synthesis, heat treatment procedures, and wear analysis of SGI and CGI across a range of temperatures.The following can be concluded from the manuscript.

- The graphite morphology has a significant impact on the tribological behavior of SG and CG irons. SG iron, with spheroidal graphite, shows better ductility and moderate wear resistance, whereas CG iron, with vermicular graphite, demonstrates improved thermal stability and crack resistance.
- Across both rotary and linear wear evaluations, CG iron consistently demonstrates increased wear loss and frictional forces in comparison to SG iron. This behavior is largely influenced by its graphite morphology and reduced ductility.
- Wear loss in both materials increases with temperature, reaching a peak around 300°C. At 500°C, the wear continues but the rate of increase becomes more gradual, likely due to oxide layer formation and material softening. SGI exhibited up to 36% lower wear loss and 15% lower friction coefficient than CGI at 500°C
- The most rapid increase in wear occurs within the first 5 minutes of testing. This is attributed to the removal of initial surface irregularities. Beyond 15 minutes, the wear rate tends to stabilize, particularly at higher temperatures.
- Frictional forces rise with both time and temperature, with a pronounced increase observed at 500°C due to enhanced surface oxidation and thermal interactions.
- Linear sliding wear tests consistently result in higher wear and frictional forces compared to rotary tests for both SG and CG irons, due to more aggressive and repeated surface contact during reciprocating motion.
- A higher magnesium content of about 0.05% in SG iron promotes spheroidal graphite formation and enhances wear resistance, while a lower magnesium content of around 0.02% in CG iron leads to vermicular graphite and comparatively higher wear.
- Austempering treatment alters the matrix into an ausferritic structure, enhancing strength and wear resistance in both SG and CG irons, while retaining the original graphite morphology.
- At room temperature, wear loss and wear scar severity are lower in both materials compared to higher temperatures. The wear behavior becomes more intense at 200°C-300°C and tends to stabilize around 500°C.
- SG iron is more suitable for applications requiring good ductility and moderate thermal endurance, whereas CG iron is better suited for high-temperature environments where thermal resistance and dimensional stability are critical.

REFERENCES

[1] D.M. Stefanescu, Solidification and modeling of cast iron – A short history of the defining moments. Mater.Sci. Eng. A **413-414**, 322-333 (2005). DOI: https://doi.org/10.1016/j.msea.2005.08.097

[2] W.D. Callister, Materials Science and Engineering: An Introduction, 7th ed. John Wiley & Sons, New York (2007).

[3] I.C.H. Hughes, Casting, 1978 ASM International.

[4] H. Fredriksson, U. Åkerlind, Materials Processing During Casting. John Wiley & Sons Inc., Hoboken (2006). DOI: https://doi.org/10.1002/0470014940

[5] J. Sertucha, J. Lacaze, J. Serrallach, R. Suárez, F. Osuna, Effect of alloying on mechanical properties of as-cast ferritic nodular cast irons. Mater. Sci. Technol. **28**, 184-191 (2012). DOI: https://doi.org/10.1179/1743284711y.0000000077

[6] R.K. Dasgupta, D.K. Mondal, A.K. Chakrabarti, A.C. Ganguli, Microstructure and mechanical properties of as-cast ductile irons alloyed with manganese and copper. J. Mater. Eng. Perform. **21**, 1728-1736 (2012). DOI: https://doi.org/10.1007/s11665-011-0044-1

[7] Z. Fan, Y. Wang, S. Liang, H. Huang, Strengthening cast iron matrix by alloying elements with positive and negative segregation. Acta Metall. Sin. (Eng. Lett.) **10**, 329-332 (1997).

[8] D.M. Stefanescu, J.R. Davis, J. Destefani, Metals Handbook, Vol. 1: Properties and Selection – Irons, Steels and High-Performance Alloys. ASM International, Materials Park, Ohio, 100-120 (1990).

[9] M. Hafiz, Mechanical properties of SG-iron with different matrix structure. J. Mater. Sci. **36**, 1293-1300 (2001). DOI: https://doi.org/10.1023/A:1017541815076

[10] A.R. Ghaderi, M. Nili Ahmadabadi, H.M. Ghasemi, Effect of graphite morphologies on the tribological behavior of austempered cast iron. Wear **255**, 410-416 (2003). DOI: https://doi.org/10.1016/S0043-1648(03)00251-2

[11] M. Nili Ahmadabadi, H.M. Ghasemi, M. Osia, Effects of successive austempering on the tribological behavior of ductile cast iron. Wear **231**, 293-300 (1999). DOI: https://doi.org/10.1016/S0043-1648(99)00178-0

[12] S. Shanmugam, N.K. Ramisetti, R.D.K. Misra, T. Mannering, D. Panda, S. Jansto, Effect of cooling rate on the microstructure and mechanical properties of Nb-microalloyed steels. Mater. Sci. Eng. A **460-46**1, 335-343 (2007). DOI: https://doi.org/10.1016/j.msea.2007.01.060

[13] G. Cho, K. Choe, K. Lee, A. Ikenaga, Effects of alloying elements on the microstructures and mechanical properties of heavy section ductile cast iron. J. Mater. Sci. Technol. **23**, 97-101 (2007).

[14] J. Sugishita, S. Fujiyoshi, The effect of cast iron graphites on friction and wear performance I: Graphite film formation on grey cast iron surfaces. Wear **66**, 209-221 (1981). DOI: https://doi.org/10.1016/0043-1648(81)90103-6

[15] A.R. Riahi, A.T. Alpas, Wear map for grey cast iron. Wear **255**, 401-409 (2003). DOI: https://doi.org/10.1016/S0043-1648(03)00248-2

[16] B.K. Prasad, Sliding wear response of cast iron as influenced by microstructural features and test condition. Mater. Sci. Eng. A **456**, 373-385 (2007). DOI: https://doi.org/10.1016/j.msea.2006.12.013

[17] J.A. Williams, J.H. Morris, A. Ball, The effect of transfer layers on the surface contact and wear of carbon-graphite materials. Tribol. Int. **30**, 663-676 (1997). DOI: https://doi.org/10.1016/S0301-679X(97)00027-8

[18] J. Sugishita, S. Fujiyoshi, The effect of cast iron graphite on friction and wear performance III: The lubricating effect of graphite under rolling-sliding contacts. Wear **77**, 181-193 (1982). DOI: https://doi.org/10.1016/0043-1648(82)90120-5

[19] M. Gagné, R.W. Smith, Spheroidal graphite iron – structure and property relationships. J. Mater. Sci. **22** (4), 1298-1308 (1987). DOI: https://doi.org/10.1007/bf01132331

[20] Y. Hirasata, T. Takahashi, Formation mechanism of spheroidal graphite in cast iron. Trans. Jpn. Foundry Soc. **3** (2), 51-58 (1991).

[21] S. Dawson, N. Tiedje, Compacted Graphite Iron: A material solution for modern engine requirements. Int. J. Cast Met. Res. **10** (6), 327-341 (1998). DOI: https://doi.org/10.1080/13640461.1998.11819362

[22] D.M. Stefanescu, Science and Engineering of Casting Solidification. Springer, 274-278 (2009). DOI: https://doi.org/10.1007/978-0-387-74610-5

[23] R. Ruxanda, A.M. Samuel, F.H. Samuel, Comparative microstructural analysis of SG and CG iron. Mater. Charact. **45** (3), 203-217 (2000). DOI: https://doi.org/10.1016/S1044-5803(00)00058-7

[24] E. Dorazil, High Strength Cast Irons. Elsevier Applied Science, 45-53 (1991).

[25] N. Tiedje, C. Ravn, Solidification and microstructure of compacted graphite iron. Int. J. Cast Met. Res. **17** (5), 298-305 (2004). DOI: https://doi.org/10.1179/136404604225021406

[26] S. Dawson, Compacted Graphite Iron for Diesel Engine Cylinder Blocks. AFS Trans. **107**, 381-388 (1999).

[27] S.K. Heibel, M. Lentz, G. Lütjering, The ausferritic transformation in ductile iron. J. Mater. Sci. Technol. **28** (3), 236-243 (2012). DOI: https://doi.org/10.1016/S1005-0302(12)60048-5

[28] D. Myszka, D. Janicki, Microstructure and mechanical properties of austempered compacted graphite iron. Arch. Foundry Eng. **14** (3), 59-64 (2014). DOI: https://doi.org/10.2478/afe-2014-0055

[29] R.B. Gundlach, J.F. Janowak, Structure–property relationships in austempered ductile irons. AFS Trans. **89**, 377-390 (1981).

[30] A. Trudel, M. Gagné, High-performance applications of ADI and ACGI. J. Mater. Eng. Perform. **15** (5), 591-596 (2006). DOI: https://doi.org/10.1361/105994906X124559

[31] M. Campos, U. de la Torre, A. Bedolla-Jacuinde, Effect of austempering time on the mechanical properties of compacted graphite iron. Mater. Sci. Eng. A **678**, 28-36 (2016). DOI: https://doi.org/10.1016/j.msea.2016.09.084

[32] Y. Lu, I. Baker, P.J. Blau, F.E. Kennedy, P.R. Munroe, A comparison of dry sliding wear of Fe30Ni20Mn25Al25 at room temperature and elevated temperature. Intermetallics **39**, 94-103 (2013). DOI: https://doi.org/10.1016/j.intermet.2013.03.013

[33] C. Rynio, H. Hattendorf, J. Klöwer, G. Eggeler, The evolution of tribo-layers during high temperature sliding wear. Wear **315** (1-2), 1-10 (2014). DOI: https://doi.org/10.1016/j.wear.2014.04.003

[34] S.K. Shaha, M.M. Haque, Effect of temperature on wear characteristic of cast iron. Thermal Spray 2010: Proc. Int. Thermal Spray Conf., Singapore, May 3-5 (2010).

[35] S. Venugopal Rao, M. Venkataramana, A.C.S. Kumar, Friction and dry sliding wear properties of compact graphite iron at room temperature and 100°C. Mater. Today Proc. **45** (2), 3250-3254 (2021). DOI: https://doi.org/10.1016/j.matpr.2020.11.150

[36] K. Hirasata, K. Hayashi, Y. Inamoto, Friction and wear of several kinds of cast irons under severe sliding conditions. Wear **263**, 790-800 (2007). DOI: https://doi.org/10.1016/j.wear.2006.12.031